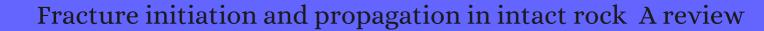
## CITATION REPORT List of articles citing



DOI: 10.1016/j.jrmge.2014.06.001 Journal of Rock Mechanics and Geotechnical Engineering, 2014, 6, 287-300.

Source: https://exaly.com/paper-pdf/59453922/citation-report.pdf

Version: 2024-04-28

This report has been generated based on the citations recorded by exaly.com for the above article. For the latest version of this publication list, visit the link given above.

The third column is the impact factor (IF) of the journal, and the fourth column is the number of citations of the article.

| #   | Paper   | IF  | Citations |
|-----|---|-----|-----------|
| 399 | Editorial. Journal of Rock Mechanics and Geotechnical Engineering, <b>2015</b> , 7, 359-360   | 5.3 | O         |
| 398 | Crack propagation and coalescence of brittle rock-like specimens with pre-existing cracks in compression. <b>2015</b> , 187, 113-121  |     | 201       |
| 397 | A refined micromechanical damage <b>f</b> riction model with strength prediction for rock-like materials under compression. <b>2015</b> , 60-61, 75-83  |     | 62        |
| 396 | A theoretical derivation of the Hoek <b>B</b> rown failure criterion for rock materials. <i>Journal of Rock Mechanics and Geotechnical Engineering</i> , <b>2015</b> , 7, 361-366   | 5.3 | 46        |
| 395 | Computing in-situ strength of rock masses based upon RQD and modified joint factor: Using pressure and damage sensitive constitutive relationship. <i>Journal of Rock Mechanics and Geotechnical Engineering</i> , <b>2015</b> , 7, 540-565 | 5.3 | 13        |
| 394 | Model for fracture initiation and propagation pressure calculation in poorly consolidated sandstone during waterflooding. <b>2015</b> , 22, 279-291   |     | 8         |
| 393 | Triaxial compression experiments on intact veined andesite. <i>International Journal of Rock Mechanics and Minings Sciences</i> , <b>2016</b> , 86, 179-193   | 6   | 16        |
| 392 | Volcaniclastic dykes tell on fracturing, explosive eruption and lateral collapse at Stromboli volcano (Italy). <b>2016</b> , 318, 55-72   |     | 5         |
| 391 | Statistical Characterization of the Mechanical Parameters of Intact Rock Under Triaxial Compression: An Experimental Proof of the Jinping Marble. <i>Rock Mechanics and Rock Engineering</i> , <b>2016</b> , 49, 4631-4646                  | 5.7 | 17        |
| 390 | Fracture Mechanics in Ancient Egypt. <b>2016</b> , 2, 2921-2928   |     | 4         |
| 389 | Discontinuum Modelling Approach for Stress Analysis at a Seismic Source: Case Study. <i>Rock Mechanics and Rock Engineering</i> , <b>2016</b> , 49, 4749-4765   | 5.7 | 8         |
| 388 | Rock Cracking Indices for Improved Tunnel Support Design: A Case Study for Columnar Jointed Rock Masses. <i>Rock Mechanics and Rock Engineering</i> , <b>2016</b> , 49, 2115-2130   | 5.7 | 27        |
| 387 | Back analysis of a pillar monitoring experiment at 2.4 km depth in the Sudbury Basin, Canada. <i>International Journal of Rock Mechanics and Minings Sciences</i> , <b>2016</b> , 85, 33-51   | 6   | 35        |
| 386 | Strength prediction of dry and saturated brittle rocks by unilateral damage-friction coupling analyses. <i>Computers and Geotechnics</i> , <b>2016</b> , 73, 16-23  | 4.4 | 16        |
| 385 | Occurrence of Foreshocks in Large Earthquakes with Strike-Slip Rupturing. <b>2016</b> , 106, 213-224  |     | 6         |
| 384 | Numerical Investigation of the Effect of the Location of Critical Rock Block Fracture on Crack Evolution in a Gob-side Filling Wall. <i>Rock Mechanics and Rock Engineering</i> , <b>2016</b> , 49, 1041-1058                               | 5.7 | 77        |
| 383 | Cementation of sand due to salt precipitation in drying process. 2017, 35, 441-445  |     | 11        |

## (2017-2017)

| 382   | Direct Shear Tests of Sandstone Under Constant Normal Tensile Stress Condition Using a Simple Auxiliary Device. <i>Rock Mechanics and Rock Engineering</i> , <b>2017</b> , 50, 1425-1438   | 5.7        | 28                          |
|---|--|------------|-----------------------------|
| 381   | Post-yield Strength and Dilatancy Evolution Across the Brittle <b>D</b> uctile Transition in Indiana Limestone. <i>Rock Mechanics and Rock Engineering</i> , <b>2017</b> , 50, 1691-1710   | 5.7        | 45                          |
| 380   | A thermodynamics-based formulation for constitutive modelling using damage mechanics and plasticity theory. <b>2017</b> , 143, 22-39   |            | 12                          |
| 379   | Comparison of existing methods and a new tensile strength based model in estimating the Hoek-Brown constant m i for intact rocks. <b>2017</b> , 224, 87-96   |            | 22                          |
| 378   | Deep Fracturing of the Hard Rock Surrounding a Large Underground Cavern Subjected to High Geostress: In Situ Observation and Mechanism Analysis. <i>Rock Mechanics and Rock Engineering</i> , <b>2017</b> , 50, 2155-2175  | 5.7        | 50                          |
| 377   | Active Seismic Monitoring of Crack Initiation, Propagation, and Coalescence in Rock. <i>Rock Mechanics and Rock Engineering</i> , <b>2017</b> , 50, 2311-2325  | 5.7        | 40                          |
| 376   | A reply to the discussion on a calibration methodology to obtain material parameters for the representation of fracture mechanics based on discrete element simulations. <i>Computers and Geotechnics</i> , <b>2017</b> , 86, 249-251  | 4.4        | 1                           |
| 375   | In situ experimental investigation of basalt spalling in a large underground powerhouse cavern. <i>Tunnelling and Underground Space Technology</i> , <b>2017</b> , 68, 82-94   | 5.7        | 39                          |
| 374   | Effect of anisotropy and hydro-mechanical couplings on pore pressure evolution during tunnel excavation in low-permeability ground. <i>International Journal of Rock Mechanics and Minings Sciences</i> , <b>2017</b> , 97, 1-14   | 6          | 21                          |
|   |  |            |                             |
| 373   | The impact of a pressurized regional sea or global ocean on stresses on Enceladus. <b>2017</b> , 122, 1258-12  | 75         | 9                           |
| 373<br>372                                      | The impact of a pressurized regional sea or global ocean on stresses on Enceladus. <b>2017</b> , 122, 1258-12  Bonded-cluster simulation of rock-cutting using PFC2D. <b>2017</b> , 20, 1289-1301  | 75         | 9                           |
|   |  | 75<br>5·3  |                             |
| 372   | Bonded-cluster simulation of rock-cutting using PFC2D. <b>2017</b> , 20, 1289-1301  Risk of shear failure and extensional failure around over-stressed excavations in brittle rock.  |            | 11                          |
| 37 <sup>2</sup><br>37 <sup>1</sup>              | Bonded-cluster simulation of rock-cutting using PFC2D. <b>2017</b> , 20, 1289-1301  Risk of shear failure and extensional failure around over-stressed excavations in brittle rock. <i>Journal of Rock Mechanics and Geotechnical Engineering</i> , <b>2017</b> , 9, 210-225  The use of discrete fracture networks for modelling coupled geomechanical and hydrological   | 5.3        | 11 27                       |
| 37 <sup>2</sup><br>37 <sup>1</sup>              | Bonded-cluster simulation of rock-cutting using PFC2D. <b>2017</b> , 20, 1289-1301  Risk of shear failure and extensional failure around over-stressed excavations in brittle rock.  Journal of Rock Mechanics and Geotechnical Engineering, <b>2017</b> , 9, 210-225  The use of discrete fracture networks for modelling coupled geomechanical and hydrological behaviour of fractured rocks. Computers and Geotechnics, <b>2017</b> , 85, 151-176   | 5.3        | 11<br>27<br>217             |
| 37 <sup>2</sup> 37 <sup>1</sup> 37 <sup>0</sup> | Bonded-cluster simulation of rock-cutting using PFC2D. 2017, 20, 1289-1301  Risk of shear failure and extensional failure around over-stressed excavations in brittle rock.  Journal of Rock Mechanics and Geotechnical Engineering, 2017, 9, 210-225  The use of discrete fracture networks for modelling coupled geomechanical and hydrological behaviour of fractured rocks. Computers and Geotechnics, 2017, 85, 151-176  Discrete element method simulation of random Voronoi grain-based models. 2017, 20, 335-345  Forensic Excavation of Rock Masses: A Technique to Investigate Discontinuity Persistence. Rock   | 5·3<br>4·4 | 11<br>27<br>217             |
| 372<br>371<br>370<br>369<br>368                 | Bonded-cluster simulation of rock-cutting using PFC2D. 2017, 20, 1289-1301  Risk of shear failure and extensional failure around over-stressed excavations in brittle rock.  Journal of Rock Mechanics and Geotechnical Engineering, 2017, 9, 210-225  The use of discrete fracture networks for modelling coupled geomechanical and hydrological behaviour of fractured rocks. Computers and Geotechnics, 2017, 85, 151-176  Discrete element method simulation of random Voronoi grain-based models. 2017, 20, 335-345  Forensic Excavation of Rock Masses: A Technique to Investigate Discontinuity Persistence. Rock Mechanics and Rock Engineering, 2017, 50, 2911-2928  Role of natural fractures in damage evolution around tunnel excavation in fractured rocks. 2017, | 5·3<br>4·4 | 11<br>27<br>217<br>11<br>33 |

| 364 | Failure Mechanisms of Brittle Rocks under Uniaxial Compression. 2017, 47, 59-80  |       | 3   |
|-----|--|-------|-----|
| 363 | Influence of Radial Stress Gradient on Strainbursts: An Experimental Study. <i>Rock Mechanics and Rock Engineering</i> , <b>2017</b> , 50, 2659-2676   | 5.7   | 43  |
| 362 | A new global database to improve predictions of permeability distribution in crystalline rocks at site scale. <b>2017</b> , 122, 3513-3539   |       | 38  |
| 361 | Dynamic mechanical behaviors of Fangshan marble. <i>Journal of Rock Mechanics and Geotechnical Engineering</i> , <b>2017</b> , 9, 807-817  | 5.3   | 15  |
| 360 | Study of Cracking Process in Granite. 2017, 191, 1108-1116   |       | 4   |
| 359 | A New Rock Strength Criterion from Microcracking Mechanisms Which Provides Theoretical Evidence of Hybrid Failure. <i>Rock Mechanics and Rock Engineering</i> , <b>2017</b> , 50, 341-352  | 5.7   | 11  |
| 358 | Modification of rock mass strength assessment methods and their application in geotechnical engineering. <i>Bulletin of Engineering Geology and the Environment</i> , <b>2017</b> , 76, 1471-1480  | 4     | 3   |
| 357 | Polygonal grain-based distinct element modeling for mechanical behavior of brittle rock. <b>2017</b> , 41, 880   | )-898 | 17  |
| 356 | Time-dependent dilatancy for brittle rocks. <i>Journal of Rock Mechanics and Geotechnical Engineering</i> , <b>2017</b> , 9, 1054-1070   | 5.3   | 3   |
| 355 | Microstructural Evolution of Porosity and Stress During the Formation of Brittle Shear Fractures: A Discrete Element Model Study. <b>2018</b> , 123, 2228-2245   |       | 5   |
| 354 | Role of grain-size in phyllonitisation: Insights from mineralogy, microstructures, strain analyses and numerical modeling. <b>2018</b> , 112, 39-52  |       | 34  |
| 353 | Geotechnical characterisation of a weak sedimentary rock mass at CERN, Geneva. <i>Tunnelling and Underground Space Technology</i> , <b>2018</b> , 77, 249-260  | 5.7   | 6   |
| 352 | Study on crack initiation and damage stress in sandstone under true triaxial compression. <i>International Journal of Rock Mechanics and Minings Sciences</i> , <b>2018</b> , 106, 117-123   | 6     | 51  |
| 351 | Maintaining geological reality in application of GSI for design of engineering structures in rock. <b>2018</b> , 239, 282-297  |       | 35  |
| 350 | A displacement-softening contact model for discrete element modeling of quasi-brittle materials. <i>International Journal of Rock Mechanics and Minings Sciences</i> , <b>2018</b> , 104, 9-19   | 6     | 21  |
| 349 | Synthetic low-strength materials as rock substitutes for physical model studies. <b>2018</b> , 4, 273-297  |       | 5   |
| 348 | Overhanging rock slope by design: An integrated approach using rock mass strength characterisation, large-scale numerical modelling and limit equilibrium methods. <i>Journal of Rock Mechanics and Geotechnical Engineering</i> , <b>2018</b> , 10, 72-90 | 5.3   | 7   |
| 347 | Experimental Study on the Growth, Coalescence and Wrapping Behaviors of 3D Cross-Embedded Flaws Under Uniaxial Compression. <i>Rock Mechanics and Rock Engineering</i> , <b>2018</b> , 51, 1379-1400   | 5.7   | 109 |

## (2018-2018)

| 346 | Volumetric analysis of rock mass instability around haulage drifts in underground mines. <i>Journal of Rock Mechanics and Geotechnical Engineering</i> , <b>2018</b> , 10, 60-71  | 5.3 | 7  |
|-----|---|-----|----|
| 345 | Quantifying the effects of scale and heterogeneity on the confined strength of micro-defected rocks. <i>International Journal of Rock Mechanics and Minings Sciences</i> , <b>2018</b> , 102, 131-143                           | 6   | 20 |
| 344 | DEM analysis of failure mechanisms in the intact Brazilian test. <i>International Journal of Rock Mechanics and Minings Sciences</i> , <b>2018</b> , 102, 109-119   | 6   | 31 |
| 343 | Approximate solutions of finite dynamic spherical cavity-expansion models for penetration into elastically confined concrete targets. <b>2018</b> , 114, 182-193  |     | 15 |
| 342 | Finite ElementBased Stability Charts for Underground Cavities in Soft Calcarenites. 2018, 18, 04018071  |     | 13 |
| 341 | The effect of mineralogical parameters on the mechanical properties of granitic rocks. <b>2018</b> , 240, 204-2   | 225 | 21 |
| 340 | An experimental investigation on deformation and failure behavior of carbonaceous Garau shale in Lurestan Basin, west Iran: Application in shale gas development. <b>2018</b> , 55, 135-153                                     |     | 9  |
| 339 | Simulating mining-induced strata permeability changes. <b>2018</b> , 237, 208-216   |     | 30 |
| 338 | Microcracking Mechanism Analysis of Rock Failure in Diametral Compression Tests. <b>2018</b> , 30, 04018082   |     | 18 |
| 337 | Shale brittleness evaluation based on energy balance analysis of stress-strain curves. <b>2018</b> , 167, 1-19  |     | 67 |
| 336 | Experimental Study of the Triaxial Strength Properties of Hollow Cylindrical Granite Specimens Under Coupled External and Internal Confining Stresses. <i>Rock Mechanics and Rock Engineering</i> , <b>2018</b> , 51, 2015-2031 | 5.7 | 38 |
| 335 | Stress Thresholds of Crack Development and Poisson® Ratio of Rock Material at High Strain Rate. <i>Rock Mechanics and Rock Engineering</i> , <b>2018</b> , 51, 945-951  | 5.7 | 20 |
| 334 | Estimation of brittleness indices for pay zone determination in a shale-gas reservoir by using elastic properties obtained from micromechanics. <b>2018</b> , 15, 307-314   |     | 6  |
| 333 | The influence of diffusion in the fracture resistance method for wellbore strengthening: A rock mechanics approach. <b>2018</b> ,   |     | Ο  |
| 332 | Investigating the Onset of Strain Localization Within Anisotropic Shale Using Digital Volume Correlation of Time-Resolved X-Ray Microtomography Images. <b>2018</b> , 123, 7509-7528  |     | 29 |
| 331 | Investigation of static/dynamic moduli and plastic response of shale specimens. <i>International Journal of Rock Mechanics and Minings Sciences</i> , <b>2018</b> , 110, 231-245  | 6   | 15 |
| 330 | Non-linear ultrasonic monitoring of damage progression in disparate rocks. <i>International Journal of</i>  | 6   | 8  |
|     | Rock Mechanics and Minings Sciences, <b>2018</b> , 111, 33-44   |     |    |

| 328 | Subcritical Crack Growth and Progressive Failure in Carrara Marble Under Wet and Dry Conditions. <b>2018</b> , 123, 3780-3798   |     | 19  |
|-----|---|-----|-----|
| 327 | Randomly oriented cracks in a transversely isotropic material. <b>2018</b> , 150, 222-229   |     | 10  |
| 326 | Experimental Study on the Damage Evolution of Brittle Rock Under Triaxial Confinement with Full Circumferential Strain Control. <i>Rock Mechanics and Rock Engineering</i> , <b>2018</b> , 51, 3321-3341                    | 5.7 | 39  |
| 325 | A Method for Multiscale Interpretation of Fracture Processes in Carrara Marble Specimen Containing a Single Flaw Under Uniaxial Compression. <b>2018</b> , 123, 6459  |     | 27  |
| 324 | Experimental simulation investigation on rockburst induced by spalling failure in deep circular tunnels. <i>Tunnelling and Underground Space Technology</i> , <b>2018</b> , 81, 413-427                                     | 5.7 | 118 |
| 323 | Review of the Relationships between Crack Initiation Stress, Mode I Fracture Toughness and Tensile Strength of Geo-Materials. <b>2018</b> , 18, 04018136  |     | 18  |
| 322 | Shear stress triggering brittle shear fracturing of rock-like materials. <b>2018</b> , 146-147, 295-302   |     | 10  |
| 321 | An Improved Crack Initiation Stress Criterion for Brittle Rocks under Confining Stress. <b>2018</b> , 170, 02214  | 41  | 2   |
| 320 | Application of Flattened Brazilian Test to Investigate Rocks Under Confined Extension. <i>Rock Mechanics and Rock Engineering</i> , <b>2018</b> , 51, 3719-3736   | 5.7 | 11  |
| 319 | Microseismicity monitoring and failure mechanism analysis of rock masses with weak interlayer zone in underground intersecting chambers: A case study from the Baihetan Hydropower Station, China. <b>2018</b> , 245, 44-60 |     | 38  |
| 318 | Elastically-homogeneous lattice modelling of transversely isotropic rocks. <i>Computers and Geotechnics</i> , <b>2018</b> , 104, 96-108   | 4.4 | 9   |
| 317 | Understanding the fracture behavior of brittle and ductile multi-flawed rocks by uniaxial loading by digital image correlation. <i>Engineering Fracture Mechanics</i> , <b>2018</b> , 199, 438-460                          | 4.2 | 81  |
| 316 | Microseismic monitoring and deformation early warning of the underground caverns of Lianghekou hydropower station, Southwest China. <b>2019</b> , 12, 1   |     | 6   |
| 315 | Effects of Anisotropy and Saturation on Geomechanical Behavior of Mudstone. <b>2019</b> , 124, 8101-8126  |     | 6   |
| 314 | Dynamic Crack Propagation and Fracture Behavior of Pre-cracked Specimens under Impact Loading by Split Hopkinson Pressure Bar. <b>2019</b> , 2019, 1-11   |     | 4   |
| 313 | A particle mechanics approach for the dynamic strength model of the jointed rock mass considering the joint orientation. <b>2019</b> , 43, 2797-2815  |     | 17  |
| 312 | Investigation of cracking behavior and mechanism of sandstone specimens with a hole under compression. <b>2019</b> , 163, 105084  |     | 19  |
| 311 | Deformation and failure characteristics and fracture evolution of cryptocrystalline basalt. <i>Journal of Rock Mechanics and Geotechnical Engineering</i> , <b>2019</b> , 11, 990-1003                                      | 5.3 | 16  |

| 310 | Numerical simulation of failure of sandstone specimens utilizing the finite-difference continuous damage mechanics approach. <b>2019</b> , 18, 135-141   |        | 3   |
|-----|--|--------|-----|
| 309 | A comprehensive study of fracture evolution of brittle rock containing an inverted U-shaped cavity under uniaxial compression. <i>Computers and Geotechnics</i> , <b>2019</b> , 116, 103219                    | 4.4    | 20  |
| 308 | Stability charts based on the finite element method for underground cavities in soft carbonate rocks: validation through case-study applications. <b>2019</b> , 19, 2079-2095                                  |        | 7   |
| 307 | Improving Hydraulic Fracturing Performance and Interpreting Fracture Geometry Based on Drilling Measurements. <b>2019</b> ,  |        | O   |
| 306 | Comparative verification of discrete and smeared numerical approaches for the simulation of hydraulic fracturing. <b>2019</b> , 10, 1  |        | 22  |
| 305 | Patterns in complex hydraulic fractures observed by true-triaxial experiments and implications for proppant placement and stimulated reservoir volumes. <b>2019</b> , 9, 2781-2792                             |        | 9   |
| 304 | Characterization of fracture formation in organic-rich shales - An experimental and real time study of the Permian Lucaogou Formation, Junggar Basin, northwestern China. <b>2019</b> , 107, 397-406           |        | 12  |
| 303 | Rock strengths and rock failure criteria. <b>2019</b> , 85-131   |        | O   |
| 302 | PFC simulation of crack evolution and energy conversion during basalt failure process. <b>2019</b> , 16, 639-6   | 51     | 21  |
| 301 | Dynamics of Microscale Precursors During Brittle Compressive Failure in Carrara Marble. <b>2019</b> , 124, 61  | 21-613 | 920 |
| 300 | Impact of tensile strength and incident angles on a soil slope under earthquake SV-waves. <b>2019</b> , 260, 105192  |        | 7   |
| 299 | Triaxial extension tests on sandstone using a simple auxiliary apparatus. <i>International Journal of Rock Mechanics and Minings Sciences</i> , <b>2019</b> , 120, 29-40                                       | 6      | 16  |
| 298 | Rock mechanics for design of Brisbane tunnels and implications of recent thinking in relation to rock mass strength. <i>Journal of Rock Mechanics and Geotechnical Engineering</i> , <b>2019</b> , 11, 676-683 | 5.3    | 6   |
| 297 | Reliability-based design in rock engineering: Application of Bayesian regression methods to rock strength data. <i>Journal of Rock Mechanics and Geotechnical Engineering</i> , <b>2019</b> , 11, 612-627      | 5.3    | 11  |
| 296 | Propagation patterns of microseismic waves in rock strata during mining: an experimental study. <b>2019</b> , 26, 531-537  |        | 12  |
| 295 | Effects of pore-crack relative location on crack propagation in porous media using XFEM method. <i>Theoretical and Applied Fracture Mechanics</i> , <b>2019</b> , 103, 102241                                  | 3.7    | 12  |
| 294 | Mechanical Characterization of Low Permeable Siltstone under Different Reservoir Saturation Conditions: An Experimental Study. <b>2019</b> , 12, 14  |        | 12  |
| 293 | Numerical Investigation of Radial Strain-Controlled Uniaxial Compression Test of SplDiorite in Grain-Based Model. <i>Rock Mechanics and Rock Engineering</i> , <b>2019</b> , 52, 3659-3674                     | 5.7    | 5   |

| 292         | Progressive failure of brittle rocks with non-isometric flaws: Insights from acousto-optic-mechanical (AOM) data. <b>2019</b> , 42, 1787-1802  |      | 63 |
|-------------|--|------|----|
| 291         | Universal confined tensile strength of intact rock. <i>Scientific Reports</i> , <b>2019</b> , 9, 6170  | 4.9  | 27 |
| <b>29</b> 0 | Experimental simulation analysis of the process and failure characteristics of spalling in D-shaped tunnels under true-triaxial loading conditions. <i>Tunnelling and Underground Space Technology</i> , <b>2019</b> , 90, 42-61 | 5.7  | 29 |
| 289         | Experimental Study on the Shear Mechanical Behavior of Sandstone Under Normal Tensile Stress Using a New Double-Shear Testing Device. <i>Rock Mechanics and Rock Engineering</i> , <b>2019</b> , 52, 3467-3474                   | 5.7  | 11 |
| 288         | Slope reliability and back analysis of failure with geotechnical parameters estimated using Bayesian inference. <i>Journal of Rock Mechanics and Geotechnical Engineering</i> , <b>2019</b> , 11, 628-643                        | 5.3  | 18 |
| 287         | FEM-based stability charts for underground cavities in soft carbonate rocks: validation through case-study applications. <b>2019</b> ,   |      |    |
| 286         | Simulation of Fracture Coalescence in Granite via the Combined FiniteDiscrete Element Method. <i>Rock Mechanics and Rock Engineering</i> , <b>2019</b> , 52, 3213-3227   | 5.7  | 34 |
| 285         | Stress magnitudes in the Basel enhanced geothermal system. <i>International Journal of Rock Mechanics and Minings Sciences</i> , <b>2019</b> , 118, 1-20   | 6    | 15 |
| 284         | Effect of Polymer Volume Fraction on Fracture Initiation in Soft Gels at Small Length Scales. <b>2019</b> , 492-   | 498  | 13 |
| 283         | Influence of Flaw Inclination Angle on Unloading Responses of Brittle Rock in Deep Underground. <i>Geofluids</i> , <b>2019</b> , 2019, 1-16  | 1.5  | 6  |
| 282         | Study on the damage-softening constitutive model of rock and experimental verification. 2019, 35, 786  | -798 | 12 |
| 281         | The role of transgranular capability in grain-based modelling of crystalline rocks. <i>Computers and Geotechnics</i> , <b>2019</b> , 110, 161-183  | 4.4  | 44 |
| <b>2</b> 80 | Crack Initiation, Propagation, and Coalescence Experiments in Sandstone Brazilian Disks Containing Pre-Existing Flaws. <i>Advances in Civil Engineering</i> , <b>2019</b> , 2019, 1-11   | 1.3  | 2  |
| 279         | Rock Engineering: Where is the Laboratory?. Rock Mechanics and Rock Engineering, 2019, 52, 4865-4888   | 5.7  | 2  |
| 278         | A Numerical Study on the Crack Development Behavior of Rock-Like Material Containing Two Intersecting Flaws. <b>2019</b> , 7, 1223   |      | 7  |
| 277         | Numerical analysis of fracture initiation and propagation in weak porous sandstones under multiaxial loading. <b>2019</b> ,  |      |    |
| 276         | Experimental investigation of the effect of compliant pores on reservoir rocks under hydrostatic and triaxial compression stress states. <b>2019</b> , 56, 983-991   |      | 3  |
| 275         | Brittleness in the Devonian Horn River shale, British Columbia, Canada. <b>2019</b> , 62, 247-258  |      | 15 |

## (2020-2019)

| 274   | The Hoek <b>B</b> rown failure criterion and GSI <b>12</b> 018 edition. <i>Journal of Rock Mechanics and Geotechnical Engineering</i> , <b>2019</b> , 11, 445-463  | 5.3         | 241                 |
|---|--|-------------|---------------------|
| 273   | Preliminary Experimental Study of Effect of CO 2 -H 2 O Biphasic Fluid on Mechanical Behavior of Sandstone under True Triaxial Compression. <b>2019</b> , 19, 06018036   |             | 3                   |
| 272   | Investigation of Abrasion and Impact Resistance of Aggregates in Different Environments in Direh, Kermanshah, Iran. <b>2019</b> , 37, 2015-2028  |             | 1                   |
| 271   | Scalable En Echelon Shear-Fracture Aperture-Roughness Mechanism: Theory, Validation, and Implications. <b>2019</b> , 124, 957-977  |             | 13                  |
| 270   | Geological Context and Fracturing State of the Rock Massifs of the Jijelian Ledge (Northeast Algeria). <b>2019</b> , 149-152   |             |                     |
| 269   | Stress-strain response and seismic signature analysis of phyllite reservoir rocks from Blue Mountain geothermal field. <b>2019</b> , 77, 204-223   |             | 15                  |
| 268   | Study on Spectrum Characteristics and Clustering of Acoustic Emission Signals from Rock Fracture. <b>2020</b> , 39, 1133-1145  |             | 6                   |
| 267   | Anisotropy of acoustic emission in coal under the uniaxial loading condition. <b>2020</b> , 130, 109465  |             | 3                   |
| 266   | Coupled poromechanics-damage mechanics modeling of fracturing during injection in brittle rocks. <b>2020</b> , 121, 256-276  |             | 6                   |
|   |  |             |                     |
| 265   | Fault mechanics and earthquakes. <b>2020</b> , 11-80   |             | 5                   |
| 265<br>264  | Fault mechanics and earthquakes. 2020, 11-80  Incorporation of tension-compression asymmetry into plastic damage phase-field modeling of quasi brittle geomaterials. 2020, 124, 71-95  |             | 5 23                |
|   | Incorporation of tension-compression asymmetry into plastic damage phase-field modeling of   | 5.7         |                     |
| 264   | Incorporation of tension-compression asymmetry into plastic damage phase-field modeling of quasi brittle geomaterials. <b>2020</b> , 124, 71-95  Physical Model Experimental Study on Spalling Failure Around a Tunnel in Synthetic Marble. <i>Rock</i>  | <i>5</i> ·7 |                     |
| 264<br>263  | Incorporation of tension-compression asymmetry into plastic damage phase-field modeling of quasi brittle geomaterials. <b>2020</b> , 124, 71-95  Physical Model Experimental Study on Spalling Failure Around a Tunnel in Synthetic Marble. <i>Rock Mechanics and Rock Engineering</i> , <b>2020</b> , 53, 909-926  An Acoustic Emission Data-Driven Model to Simulate Rock Failure Process. <i>Rock Mechanics and Rock</i>  |             | 23                  |
| <ul><li>264</li><li>263</li><li>262</li></ul>                         | Incorporation of tension-compression asymmetry into plastic damage phase-field modeling of quasi brittle geomaterials. 2020, 124, 71-95  Physical Model Experimental Study on Spalling Failure Around a Tunnel in Synthetic Marble. Rock Mechanics and Rock Engineering, 2020, 53, 909-926  An Acoustic Emission Data-Driven Model to Simulate Rock Failure Process. Rock Mechanics and Rock Engineering, 2020, 53, 1605-1621  Fracture damage prediction in fissured red sandstone under uniaxial compression: acoustic   |             | 23 4 11             |
| 264<br>263<br>262<br>261  | Incorporation of tension-compression asymmetry into plastic damage phase-field modeling of quasi brittle geomaterials. 2020, 124, 71-95  Physical Model Experimental Study on Spalling Failure Around a Tunnel in Synthetic Marble. Rock Mechanics and Rock Engineering, 2020, 53, 909-926  An Acoustic Emission Data-Driven Model to Simulate Rock Failure Process. Rock Mechanics and Rock Engineering, 2020, 53, 1605-1621  Fracture damage prediction in fissured red sandstone under uniaxial compression: acoustic emission b-value analysis. 2020, 43, 175-190  Evaluation of an Ultrasonic Method for Damage Characterization of Brittle Rocks. Rock Mechanics   | 5.7         | 23<br>4<br>11<br>28 |
| <ul><li>264</li><li>263</li><li>262</li><li>261</li><li>260</li></ul> | Incorporation of tension-compression asymmetry into plastic damage phase-field modeling of quasi brittle geomaterials. 2020, 124, 71-95  Physical Model Experimental Study on Spalling Failure Around a Tunnel in Synthetic Marble. Rock Mechanics and Rock Engineering, 2020, 53, 909-926  An Acoustic Emission Data-Driven Model to Simulate Rock Failure Process. Rock Mechanics and Rock Engineering, 2020, 53, 1605-1621  Fracture damage prediction in fissured red sandstone under uniaxial compression: acoustic emission b-value analysis. 2020, 43, 175-190  Evaluation of an Ultrasonic Method for Damage Characterization of Brittle Rocks. Rock Mechanics and Rock Engineering, 2020, 53, 2077-2094 | 5.7         | 23<br>4<br>11<br>28 |

| 256 | Anisotropic characteristics of crack initiation and crack damage thresholds for shale. <i>International Journal of Rock Mechanics and Minings Sciences</i> , <b>2020</b> , 126, 104178  | 6   | 20 |
|-----|---|-----|----|
| 255 | Experimental study on fracture toughness of a compacted clay using semi-circular bend specimen. <i>Engineering Fracture Mechanics</i> , <b>2020</b> , 224, 106814   | 4.2 | 16 |
| 254 | A review on the experimental techniques and applications in the geomechanical evaluation of shale gas reservoirs. <b>2020</b> , 74, 103090  |     | 17 |
| 253 | Laboratory Study of the Fracturing Process in Marble and Plaster Hollow Plates Subjected to Uniaxial Compression by Combined Acoustic Emission and Digital Image Correlation Techniques. <i>Rock Mechanics and Rock Engineering</i> , <b>2020</b> , 53, 1953-1971 | 5.7 | 12 |
| 252 | Control of the Chamber in Extra-Thick Coal Seam Based on Fracture Characteristics of Coal Rock and Mass. <i>Advances in Civil Engineering</i> , <b>2020</b> , 2020, 1-13  | 1.3 | 1  |
| 251 | Experimental investigation on fracturing process of marble under biaxial compression. <i>Journal of Rock Mechanics and Geotechnical Engineering</i> , <b>2020</b> , 12, 943-959   | 5.3 | 7  |
| 250 | Influence of Deviatoric Stress on the Deformation and Damage Evolution of Surrounding Rock under Unloading Conditions. <i>Shock and Vibration</i> , <b>2020</b> , 2020, 1-14  | 1.1 | 1  |
| 249 | Research of Transitional Failure Mode as Damage Evolution in Rock Wall. <i>Advances in Civil Engineering</i> , <b>2020</b> , 2020, 1-12   | 1.3 | 1  |
| 248 | Fracture and Time-Varying Multifractal Behaviors of Single-Flawed Red Sandstone with Different Wavilness Angles. <b>2020</b> , 32, 04020272   |     | 4  |
| 247 | Three-dimensional finite-difference analysis of deformation and failure of weak porous sandstones subjected to uniaxial compression. <i>International Journal of Rock Mechanics and Minings Sciences</i> , <b>2020</b> , 133, 104412                              | 6   | 4  |
| 246 | Discrete numerical analyses of grain size influence on the fracture of notched rock beams. <i>Computers and Geotechnics</i> , <b>2020</b> , 125, 103680   | 4.4 | 3  |
| 245 | An Extension Failure Criterion for Brittle Rock. <i>Advances in Civil Engineering</i> , <b>2020</b> , 2020, 1-12  | 1.3 | 1  |
| 244 | Structural Geology: A Quantitative Introduction. <b>2020</b> , 25-69  |     |    |
| 243 | Structural Geology: A Quantitative Introduction. <b>2020</b> , 70-102   |     |    |
| 242 | Structural Geology: A Quantitative Introduction. <b>2020</b> , 379-420  |     |    |
| 241 | Structural Geology: A Quantitative Introduction. <b>2020</b> , 3-22   |     |    |
| 240 | Discrete Element Modeling of Crack Initiation Stress of Marble Based on Griffith Strength Theory. <i>Advances in Civil Engineering</i> , <b>2020</b> , 2020, 1-11   | 1.3 | 1  |
| 239 | Dynamic spherical cavity expansion analysis of concrete/rock based on Hoek-Brown criterion. <b>2020</b> , 1507, 032012  |     |    |

| 238 | Experimental verification of parameter m in Hoek <b>B</b> rown failure criterion considering the effects of natural fractures. <i>Journal of Rock Mechanics and Geotechnical Engineering</i> , <b>2020</b> , 12, 1036-1045   | 3   |
|-----|--|-----|
| 237 | New scaling of fractures in a giant carbonate platform from outcrops and subsurface. <b>2020</b> , 140, 104142   | 2   |
| 236 | The critical behaviour of finite thickness lining systems in tunnels. <b>2020</b> , 1-18   | 2   |
| 235 | Numerical investigation on crack development and energy evolution of stressed coal-rock combination. <i>International Journal of Rock Mechanics and Minings Sciences</i> , <b>2020</b> , 133, 104417   | 7   |
| 234 | Full- and Local-Field Strain Evolution and Fracture Behavior of Precracked Granite under Coupled Static and Dynamic Loads. <i>Shock and Vibration</i> , <b>2020</b> , 2020, 1-15   | 0   |
| 233 | Seismicity and Stress Associated With a Fluid-Driven Fracture: Estimating the Evolving Geometry. <b>2020</b> , 125, e2020JB020190  | 1   |
| 232 | Experimental Study on Hydro-mechanical Behaviour of Anisotropic Columnar Jointed Rock-Like Specimens. <i>Rock Mechanics and Rock Engineering</i> , <b>2020</b> , 53, 5781-5794   | 7   |
| 231 | Effect of Stress Path on the Failure Envelope of Intact Crystalline Rock at Low Confining Stress. <b>2020</b> , 10, 1119   | 5   |
| 230 | DEM simulation of the complete triaxial test of sandstone. <b>2020</b> , 570, 022027   | 1   |
| 229 | Static and coupled dynamic testing of granite for geological disposal of high-level waste. <b>2020</b> , 570, 032016   | Ο   |
| 228 | Effect of loading rate on fracture behaviors of shale under mode I loading. 2020, 27, 3118-3132  | 7   |
| 227 | Development of a semi-quantitative risk matrix for strain-burst hazard assessment IA numerical modelling approach in the absence of micro-seismic data. <b>2020</b> , 279, 105893  | 2   |
| 226 | Elastic and Frictional Properties of Fault Zones in Reservoir-Scale Hydro-Mechanical Models Machanical Machanical Models Machanical Mac | 0   |
| 225 | Breakage process of mineral processing comminution machines [An approach to liberation. <b>2020</b> , 31, 3669-3685  | 7   |
| 224 | A Semi-empirical Failure Criterion for Brittle Rocks. <i>Rock Mechanics and Rock Engineering</i> , <b>2020</b> , 53, 4271 4277   | 7 1 |
| 223 | Swelling and embedment induced by sub- and super-critical-CO2 on the permeability of propped fractures in shale. <b>2020</b> , 225, 103496   | 6   |
| 222 | Illumination of Damage in Intact Rocks by Ultrasonic Transmission-Reflection and Digital Image Correlation. <b>2020</b> , 125, e2020JB019526   | 4   |
| 221 | Simulation of mixed-mode fracture using the combined finitediscrete element method. <b>2020</b> , 7, 1047-1055   | 4   |

| 220 | Faults as Volumetric Weak Zones in Reservoir-Scale Hydro-Mechanical Finite Element Models A Comparison Based on Grid Geometry, Mesh Resolution and Fault Dip. <b>2020</b> , 13, 2673  |     | 2  |
|-----|---|-----|----|
| 219 | Influence of the porosity on the uniaxial compressive strength of sandstone samples. <b>2020</b> , 25, 465-469  |     | О  |
| 218 | Crack initiation of granite under uniaxial compression tests: A comparison study. <i>Journal of Rock Mechanics and Geotechnical Engineering</i> , <b>2020</b> , 12, 656-666   | 5.3 | 16 |
| 217 | Comparative Investigation on the CompressionBhear and TensionBhear Behaviour of Sandstone at Different Shearing Rates. <i>Rock Mechanics and Rock Engineering</i> , <b>2020</b> , 53, 3111-3131                                 | 5.7 | 8  |
| 216 | Deformation localization and cracking processes of sandstone containing two flaws of different geometric arrangements. <b>2020</b> , 43, 1959-1977  |     | 8  |
| 215 | A new method for assessing slope unloading zones based on unloading strain. <b>2020</b> , 79, 1   |     | 4  |
| 214 | Influence of crystal structure on constitutive anisotropy of silica sand at particle-scale. <i>Computers and Geotechnics</i> , <b>2020</b> , 126, 103718  | 4.4 | 7  |
| 213 | Numerical study on the progressive failure of heterogeneous geomaterials under varied confining stresses. <b>2020</b> , 269, 105556   |     | 6  |
| 212 | Creep and permeability evolution behavior of red sandstone containing a single fissure under a confining pressure of 30 MPa. <i>Scientific Reports</i> , <b>2020</b> , 10, 1900   | 4.9 | 13 |
| 211 | A generalized power-law criterion for rocks based on Mohr failure theory. <i>International Journal of Rock Mechanics and Minings Sciences</i> , <b>2020</b> , 128, 104274   | 6   | 1  |
| 210 | Investigating the crack initiation and propagation mechanism in brittle rocks using grain-based finite-discrete element method. <i>International Journal of Rock Mechanics and Minings Sciences</i> , <b>2020</b> , 127, 104219 | 6   | 43 |
| 209 | A Simple Time-Dependent Chart of Extension Fracture Initiation within Brittle Homogenous and Heterogeneous Rock Pillars in Hard Rock Mining. <b>2020</b> , 38, 2803-2833  |     | 5  |
| 208 | Acoustic Emission Characteristics and Damage Evolution of Coal at Different Depths Under Triaxial Compression. <i>Rock Mechanics and Rock Engineering</i> , <b>2020</b> , 53, 2063-2076   | 5.7 | 39 |
| 207 | Numerical simulation of roof cavings in several Kuzbass mines using finite-difference continuum damage mechanics approach. <i>International Journal of Mining Science and Technology</i> , <b>2020</b> , 30, 157-166            | 7.1 | 14 |
| 206 | Fracture Mechanism of the Formation with a Natural Flaw Under a Single-Tooth Cutting. <b>2020</b> , 33, 719-7   | '30 | 0  |
| 205 | Depth of penetration of steel-tube-confined concrete targets based on dynamic finite cylindrical cavity-expansion models. <b>2020</b> , 2, 1  |     | 1  |
| 204 | Fluid-driven fractures in granular media: Insights from numerical investigations. <b>2020</b> , 101, 042903   |     | 6  |
| 203 | Evaluation of methods for determining rock brittleness under compression. <b>2020</b> , 78, 103321  |     | 9  |

| 202 | Flat-joint model to reproduce the mechanical behaviour of intact rocks. <b>2021</b> , 25, 1427-1448  |      | 22  |
|-----|--|------|-----|
| 201 | The penetration of limestone targets by rigid projectiles: Revisited. <b>2021</b> , 12, 110-125  |      | О   |
| 200 | The damage-failure criteria for numerical stability analysis of underground excavations: A review. <i>Tunnelling and Underground Space Technology</i> , <b>2021</b> , 107, 103633                                      | 5.7  | 9   |
| 199 | A continuum grain-based model for intact and granulated Wombeyan marble. <i>Computers and Geotechnics</i> , <b>2021</b> , 129, 103872  | 4.4  | 5   |
| 198 | The mechanical behaviour of pre-existing transverse cracks in lignite under uniaxial compression. <b>2021</b> , 7, 1   |      | 0   |
| 197 | Experimental investigation on splitting failure of high sidewall cavern under three-dimensional high in-situ stress. <i>Tunnelling and Underground Space Technology</i> , <b>2021</b> , 108, 103725                    | 5.7  | 4   |
| 196 | Three-Dimensional Crack Recognition by Unsupervised Machine Learning. <i>Rock Mechanics and Rock Engineering</i> , <b>2021</b> , 54, 893-903   | 5.7  | 10  |
| 195 | Elastic and Thermoelastic Effects on Thermal Water Convection in Fracture Zones. <b>2021</b> , 126, e2020JB0   | 2094 | 0 1 |
| 194 | Experimental investigation on gas permeability in bedding shale with brittle and semi-brittle deformations under triaxial compression. <b>2021</b> , 196, 108049   |      | 7   |
| 193 | Investigation of the anisotropic confinement-dependent brittleness of a Utah coal. <b>2020</b> , 8, 274-290  |      | 11  |
| 192 | Brittle-ductile failure transition in geomaterials modeled by a modified phase-field method with a varying damage-driving energy coefficient. <b>2021</b> , 136, 102836  |      | 11  |
| 191 | Failure characteristics of surrounding rocks along the radial direction of underground excavations: An experimental study. <b>2021</b> , 281, 105984   |      | 3   |
| 190 | Influence of Weathering on the Strength and Hoek <b>B</b> rown Parameters of a Kinzigite Gneiss. <b>2021</b> , 39, 3995-4008   |      | О   |
| 189 | Identification, segregation, and characterization of individual cracks in three dimensions.  International Journal of Rock Mechanics and Minings Sciences, 2021, 138, 104615   | 6    | 1   |
| 188 | Experimental investigation on infrared radiation features of fracturing process in jointed rock under concentrated load. <i>International Journal of Rock Mechanics and Minings Sciences</i> , <b>2021</b> , 139, 1046 | 19   | 5   |
| 187 | A novel test device for the direct measurement of tensile strength of rock using ring shape sample. <i>International Journal of Rock Mechanics and Minings Sciences</i> , <b>2021</b> , 139, 104649                    | 6    | 4   |
| 186 | Lattice strain during compressive loading of AlCrFeNiTi multi-principal element alloys. <b>2021</b> , 33, 1541-1   | 554  | 1   |
| 185 | Origin of Strong Nonlinear Dependence of Fracture (Joint) Spacing on Bed Thickness in Layered Rocks: Mechanical Analysis and Modeling. <b>2021</b> , 126, e2020JB020656  |      | 1   |

| 184 | Failure in Confined Brazilian Tests on Sandstone. Applied Sciences (Switzerland), 2021, 11, 2285   | 2.6 | 1  |
|-----|--|-----|----|
| 183 | Effect of the number of coplanar rock bridges on the shear strength and stability of slopes with the same discontinuity persistence. <i>Bulletin of Engineering Geology and the Environment</i> , <b>2021</b> , 80, 3675-369                         | 91  | 1  |
| 182 | Mechanical properties and fracture behavior of flawed granite under dynamic loading. <b>2021</b> , 142, 1065   | 69  | 2  |
| 181 | Mechanical response of the Middle Bakken rocks under triaxial compressive test and nanoindentation. <i>International Journal of Rock Mechanics and Minings Sciences</i> , <b>2021</b> , 139, 104660  | 6   | 2  |
| 180 | Investigation of Microcrack Propagation and Energy Evolution in Brittle Rocks Based on the Voronoi Model. <i>Materials</i> , <b>2021</b> , 14,   | 3.5 | 2  |
| 179 | Surface-Mounted Bare and Packaged Fiber Bragg Grating Sensors for Measuring Rock Strain in Uniaxial Testing. <b>2021</b> , 21,   |     | 2  |
| 178 | Cracking behaviors and chaotic characteristics of sandstone with unfilled and filled dentate flaw. <i>Theoretical and Applied Fracture Mechanics</i> , <b>2021</b> , 112, 102876   | 3.7 | 10 |
| 177 | Ground surface rock buckling: analysis of collected cases and failure mechanisms. <i>Bulletin of Engineering Geology and the Environment</i> , <b>2021</b> , 80, 4255-4276   | 4   | O  |
| 176 | Tflerin Hoek-Brown Sabitinin (mi) Belirlenmesi iিh Bir Deneysel विl⊞ha.  |     |    |
| 175 | Experimental study on strength properties, fracture patterns, and permeability behaviors of sandstone containing two filled fissures under triaxial compression. <i>Bulletin of Engineering Geology and the Environment</i> , <b>2021</b> , 80, 5921 | 4   | 4  |
| 174 | Geomechanical conditions of extraction of gold-bearing ore reserves under the bottom of an open pit mine in Malomyr quartz deposit. <b>2021</b> , 773, 012085  |     |    |
| 173 | The Strength of Massive to Moderately Jointed Rock and its Application to Cave Mining. <i>Rock Mechanics and Rock Engineering</i> , <b>2021</b> , 54, 3629-3661  | 5.7 | 3  |
| 172 | Mechanisms of tripartite permeability evolution for supercritical CO2 in propped shale fractures. <b>2021</b> , 292, 120188  |     | 3  |
| 171 | Anisotropic energy-based progressive damage model for laminated geomaterials. <b>2021</b> , 93, 563-577  |     | 5  |
| 170 | Effect of shear bond failure on the strength ratio in DEM modeling of quasi-brittle materials. <i>Acta Geotechnica</i> , <b>2021</b> , 16, 2629-2642   | 4.9 | 2  |
| 169 | Dynamic finite cylindrical cavity-expansion models for cellular steel tube confined concrete targets normally impacted by rigid sharp-nosed projectiles. 204141962110272   |     |    |
| 168 | Simulation of the rock meso-fracturing process adopting local multiscale high-resolution modeling. <i>International Journal of Rock Mechanics and Minings Sciences</i> , <b>2021</b> , 142, 104753   | 6   | 0  |
| 167 | Evolution of Permeability in Sandstone During Confined Brazilian Testing. <i>Rock Mechanics and Rock Engineering</i> , 1   | 5.7 | 1  |

| 166 | COMPARISON OF PREDICTED FAILURE AREA AROUND THE BOREHOLES IN THE STRIKE-SLIP FAULTING STRESS REGIME WITH HOEK-BROWN AND FAIRHURST GENERALIZED CRITERIA. <b>2021</b> , 27, 346-354  |     | 4  |
|-----|--|-----|----|
| 165 | Characterization of Hoek <b>B</b> rown constant mi of quasi-isotropic intact rock using rigidity index approach. <i>Acta Geotechnica</i> , 1   | 4.9 | О  |
| 164 | The fold-thrust belt stress cycle: Superposition of normal, strike-slip, and thrust faulting deformation regimes. <b>2021</b> , 148, 104362  |     | 10 |
| 163 | New insights into the fracture mechanism of flattened Brazilian disc specimen using digital image correlation. <i>Engineering Fracture Mechanics</i> , <b>2021</b> , 252, 107810   | 4.2 | 8  |
| 162 | Fracture behaviours of brittle ceramics under elliptical ultrasonic vibration: near-to-limit contact analysis of an elastic flat punch. 1  |     | 2  |
| 161 | A modified cohesive damage-plasticity model for distinct lattice spring model on rock fracturing. <i>Computers and Geotechnics</i> , <b>2021</b> , 135, 104152   | 4.4 | 2  |
| 160 | Investigations of Coal-Rock Parting-Coal Structure (CRCS) Slip and Instability by Excavation. <i>Shock and Vibration</i> , <b>2021</b> , 2021, 1-15  | 1.1 | 0  |
| 159 | An Extension Strain Type Mohrtoulomb Criterion. Rock Mechanics and Rock Engineering, 2021, 1   | 5.7 | O  |
| 158 | Crack Initiation Evolution Under Triaxial Loading Conditions. <b>2021</b> , 833, 012012  |     | 1  |
| 157 | The Mechanism of Rock Mass Crack Propagation of Principal Stress Rotation in the Process of Tunnel Excavation. <i>Shock and Vibration</i> , <b>2021</b> , 2021, 1-12   | 1.1 | 1  |
| 156 | Research on Microscopic Evolution Laws of Sandstone Deformation and Failure Based on the Particle Discrete Element Method. <b>2021</b> , 2021, 1-12  |     |    |
| 155 | The material-structure duality of rock mass: Insight from numerical modeling. <i>International Journal of Rock Mechanics and Minings Sciences</i> , <b>2021</b> , 144, 104821  | 6   | 5  |
| 154 | Deformation and Failure Parameters of Cement-Modified Loess: Application to the Calculation of the Safety Factor of a Road Structure. <b>2022</b> , 229-241  |     |    |
| 153 | Failure in the Tension Zone around a Circular Tunnel Excavated in Saturated Porous Rock. <i>Applied Sciences (Switzerland)</i> , <b>2021</b> , 11, 8384  | 2.6 | O  |
| 152 | Progressive Failure Process of Anisotropic Rock: Insight from Full-Field Strain Evolution. 1   |     | 0  |
| 151 | Brittle-Ductile Transition and Hoek <b>B</b> rown mi Constant of Low-Porosity Carbonate Rocks. 1   |     | O  |
| 150 | Development of a 3-D confinement-dependent dilation model for brittle rocks; Part 1, derivation of a Cartesian plastic strain increments ratios approach for non-potential flow rules. <i>International Journal of Rock Mechanics and Minings Sciences</i> , <b>2021</b> , 145, 104668 | 6   | 1  |
| 149 | Safety factor calculation of a road structure with cement-modified loess as subgrade. <b>2021</b> , 30, 100604   |     | O  |

| 148 | An investigation on prevalent strategies for XFEM-based numerical modeling of crack growth in porous media. <b>2021</b> , 15, 914  |     | O  |
|-----|--|-----|----|
| 147 | Study on Rockburst Proneness of Deep Tunnel Under Different Geo-Stress Conditions Based on DEM. 1  |     | O  |
| 146 | Advances in the understanding of the role of degree of saturation and water distribution in mechanical behaviour of calcarenites using magnetic resonance imaging technique. <b>2021</b> , 303, 124420                       |     | 1  |
| 145 | Microseismic monitoring to assess rock mass damaging through a novel damping ratio-based approach. <i>International Journal of Rock Mechanics and Minings Sciences</i> , <b>2021</b> , 146, 104883                           | 6   | 2  |
| 144 | Durability prediction of brittle rocks based on type-I crack extension theory. <i>Theoretical and Applied Fracture Mechanics</i> , <b>2021</b> , 115, 103044   | 3.7 | O  |
| 143 | Morphological features and fractography analysis for in situ spalling in the China Jinping underground laboratory with a 2400 m burial depth. <i>Tunnelling and Underground Space Technology</i> , <b>2021</b> , 118, 104194 | 5.7 | 2  |
| 142 | Ultrasonic prediction of crack density using machine learning: A numerical investigation. <b>2022</b> , 13, 1012   | 77  | Ο  |
| 141 | In situ observation of spalling process of intact rock mass at large cavern excavation. <b>2017</b> , 226, 52-69   |     | 41 |
| 140 | Structural Geology: A Quantitative Introduction. <b>2020</b> ,   |     | 5  |
| 139 | The 3D stress state from geomechanicalflumerical modelling and its uncertainties: a case study in the Bavarian Molasse Basin. <b>2020</b> , 8,   |     | 6  |
| 138 | Internal Morphology of Cracking of Two 3-D Pre-Existing Cross-Embedded Flaws under Uniaxial Compression. <b>2018</b> , 41, 20170189  |     | 21 |
| 137 | Progressive Damage of a Canadian Granite in Laboratory Compression Tests and Underground Excavations. <b>2021</b> , 11, 10   |     | 2  |
| 136 | Numerical and experimental studies on the effect of loading angle on the validity of flattened Brazilian disc test. <b>2016</b> , 8, 1-12  |     | 4  |
| 135 | Experimental investigation on the penetration characteristics of low-frequency impact of pulsed water jet. <b>2022</b> , 488-489, 204145   |     | 1  |
| 134 | Universal precursor seismicity pattern before locked-segment rupture and evolutionary rule for landmark earthquakes. <b>2021</b> , 13, 101314  |     | 1  |
| 133 | Creep Rupture and Permeability Evolution in High Temperature Heat-Treated Sandstone Containing Pre-Existing Twin Flaws. <b>2021</b> , 14, 6362   |     | 1  |
| 132 | Extended finite element method simulation and experimental test on failure behavior of defects under uniaxial compression. 1-16  |     | 2  |
| 131 | Forty-Year Review of the Hoek <b>B</b> rown Failure Criterion for Jointed Rock Masses. <i>Rock Mechanics and Rock Engineering</i> , <b>2022</b> , 55, 439  | 5.7 | 2  |

| 130 | The effect of true-triaxial stress path on induced fracturing in anisotropic gneiss. 2016, 79-90  | 1 |
|-----|---|---|
| 129 | Polygonal Grain-Based Distinct Element Modelling of Mechanical Characteristics and Transverse Isotropy of Rock. <b>2016</b> , 26, 235-252                                     |   |
| 128 | Discussions on Correction of Goodman Jack Test. <b>2017</b> , 40, 20160121  |   |
| 127 | Calibration of a Distinct Element Model for Rock Considering the Residual Strength. <b>2018</b> , 48-56   |   |
| 126 | Calibrating the Strength Ratio and the Failure Envelope for DEM Modeling of Quasi-Brittle Materials. <b>2018</b> , 199-202  |   |
| 125 | Geomechanical Investigation of High Priority Geothermal Strata in the Molasse Basin, Bavaria, Germany. <b>2019</b> , 21-26  | O |
| 124 | Structural Geology: A Quantitative Introduction. <b>2020</b> , 184-220  |   |
| 123 | Structural Geology: A Quantitative Introduction. <b>2020,</b> xv-xvii   |   |
| 122 | Structural Geology: A Quantitative Introduction. <b>2020</b> , 301-345  |   |
| 121 | Structural Geology: A Quantitative Introduction. <b>2020</b> , x-xiv  |   |
| 120 | Structural Geology: A Quantitative Introduction. <b>2020</b> , 103-220  |   |
| 119 | Structural Geology: A Quantitative Introduction. <b>2020</b> , 223-257  |   |
| 118 | Influence of heterogeneity, natural fracture, and bedding plane on fracture propagation in the vicinity of a borehole. <b>2021</b> , 861, 032001                              |   |
| 117 | Comparison of H-B and M-C Failure Criterion at Low Confinement and their Impact on the Prediction of Failure Zone Around an Underground Metal Mine. <b>2021</b> , 861, 022022 |   |
| 116 | Analysis of rockburst driving mechanism based on unbalanced force. <b>2021</b> , 861, 032047  | 1 |
|     |   |   |
| 115 | Experimental investigation on dynamic mechanical behavior and fracture evolution of fissure-filled red sandstone after thermal treatment. <b>2021</b> , 106433                | O |
| 115 | Experimental investigation on dynamic mechanical behavior and fracture evolution of fissure-filled  |   |

| 112 | Evolution of Gas Permeability of Rock Salt Under Different Loading Conditions and Implications on the Underground Hydrogen Storage in Salt Caverns. <i>Rock Mechanics and Rock Engineering</i> , 1 | 5.7 | O |
|-----|--|-----|---|
| 111 | Energy Partitioning, Dynamic Fragmentation, and Off-Fault Damage in the Earthquake Source Volume. <b>2021</b> , 126, e2021JB022616   |     | 1 |
| 110 | Effects of Flaw Geometry on the Fracturing Behavior of Rock-Like Materials Containing Two Arch-Like Parallelogram Flaws. <i>Advances in Civil Engineering</i> , <b>2020</b> , 2020, 1-15           | 1.3 |   |
| 109 | Review of Parameter Inversion Approaches in Meso Constitutive Models for Rock Brittle Materials. <b>2020</b> , 09, 61-69   |     |   |
| 108 | Experimental Investigation on the Initiation of Hydraulic Fractures from a Simulated Wellbore in Laminated Shale. <b>2021</b> , 2021,  |     | 0 |
| 107 | Structural Geology: A Quantitative Introduction. <b>2020</b> , 144-183   |     |   |
| 106 | Structural Geology: A Quantitative Introduction. <b>2020</b> , 221-420   |     |   |
| 105 | Structural Geology: A Quantitative Introduction. <b>2020</b> , 105-143   |     |   |
| 104 | Structural Geology: A Quantitative Introduction. <b>2020</b> , 346-378   |     |   |
| 103 | Structural Geology: A Quantitative Introduction. <b>2020</b> , xviii-xviii   |     |   |
| 102 | Structural Geology: A Quantitative Introduction. <b>2020</b> , 23-102  |     |   |
| 101 | Structural Geology: A Quantitative Introduction. <b>2020</b> , 1-22  |     |   |
| 100 | Structural Geology: A Quantitative Introduction. <b>2020</b> , 421-427   |     |   |
| 99  | Structural Geology: A Quantitative Introduction. <b>2020</b> , 258-300   |     |   |
| 98  | Index. <b>2020</b> , 428-434   |     |   |
| 97  | Calibration and uniqueness analysis of microparameters for DEM cohesive granular material. <i>International Journal of Mining Science and Technology</i> , <b>2021</b> , 32, 121-121               | 7.1 | 4 |
| 96  | Effects of amygdale heterogeneity and sample size on the mechanical properties of basalt. <i>Journal of Rock Mechanics and Geotechnical Engineering</i> , <b>2021</b> ,                            | 5.3 | О |
| 95  | The Influence of Loading Rate on Direct and Indirect Tensile Strengths: Laboratory and Numerical Methods. <i>Shock and Vibration</i> , <b>2021</b> , 2021, 1-17                                    | 1.1 |   |

| 94   | Energy Characteristics of Acoustic Emission at the Volume-Expansion Point of a Rock Bridge: A New Insight into the Evolutionary Mechanism of Coastal Cliff Collapse. <i>Journal of Marine Science and Engineering</i> , <b>2021</b> , 9, 1338   | 2.4                      |        |
|--|---|--------------------------|--------|
| 93   | Rock Failure and Instability from a Structural Perspective: Insights from the Shape Effect. <i>Rock Mechanics and Rock Engineering</i> , 1  | 5.7                      | 1      |
| 92   | A crack theory-based bonded particle model for rock particles considering size effect on crushing strength. <i>Geotechnique Letters</i> , <b>2021</b> , 11, 1-38  | 1.7                      | 0      |
| 91   | A new discrete element model for rock-like materials. <i>Computers and Structures</i> , <b>2022</b> , 261-262, 106730   | 4.5                      | 2      |
| 90   | A systematic methodology to calibrate wellbore failure models, estimate the in-situ stress tensor and evaluate wellbore cross-sectional geometry. <i>International Journal of Rock Mechanics and Minings Sciences</i> , <b>2022</b> , 149, 104935   | 6                        | О      |
| 89   | Fracture analysis of central-flawed rock-like specimens under the influence of coplanar or non-coplanar edge flaws. <i>Bulletin of Engineering Geology and the Environment</i> , <b>2022</b> , 81, 1  | 4                        | 3      |
| 88   | Estimation of Mechanical Properties of the Bakken Shales Through Convolutional Neural Networks. <i>Rock Mechanics and Rock Engineering</i> , <b>2022</b> , 55, 1213   | 5.7                      |        |
| 87   | Rock grain-scale mechanical properties influencing hydraulic fracturing using Hydro-GBM approach. <i>Engineering Fracture Mechanics</i> , <b>2022</b> , 262, 108227   | 4.2                      | 2      |
| 86   | A damage bond model to investigate the damage and crack propagation for cemented materials and parametric analysis. <i>Materials and Structures/Materiaux Et Constructions</i> , <b>2021</b> , 54, 1  | 3.4                      | 1      |
|  |   |                          |        |
| 85   | Results. Springer Theses, <b>2022</b> , 103-191   | 0.1                      |        |
| 8 <sub>5</sub>                                     | Results. <i>Springer Theses</i> , <b>2022</b> , 103-191  Wellbore/borehole stability in shale formation. <b>2022</b> , 125-154  | 0.1                      |        |
|  |   | 0.1                      |        |
| 84   | Wellbore/borehole stability in shale formation. <b>2022</b> , 125-154  Testing and Numerical Simulations on Fracture Behavior of Fresh Quartzite Rock Using the Discrete  |                          |        |
| 84   | Wellbore/borehole stability in shale formation. 2022, 125-154  Testing and Numerical Simulations on Fracture Behavior of Fresh Quartzite Rock Using the Discrete Element Method. Lecture Notes in Mechanical Engineering, 2022, 183-193   | 0.4                      | 2      |
| 8 <sub>4</sub><br>8 <sub>3</sub><br>8 <sub>2</sub> | Wellbore/borehole stability in shale formation. 2022, 125-154  Testing and Numerical Simulations on Fracture Behavior of Fresh Quartzite Rock Using the Discrete Element Method. Lecture Notes in Mechanical Engineering, 2022, 183-193  Rock Mechanical Basics. Springer Theses, 2022, 21-44  Mechanical and Fracture Behaviors of Brittle Material with a Circular Inclusion: Insight from Infilling  | 0.4                      | 2      |
| 84<br>83<br>82<br>81                               | Wellbore/borehole stability in shale formation. 2022, 125-154  Testing and Numerical Simulations on Fracture Behavior of Fresh Quartzite Rock Using the Discrete Element Method. Lecture Notes in Mechanical Engineering, 2022, 183-193  Rock Mechanical Basics. Springer Theses, 2022, 21-44  Mechanical and Fracture Behaviors of Brittle Material with a Circular Inclusion: Insight from Infilling Composition. Rock Mechanics and Rock Engineering, 1  Geomechanische Reservoircharakterisierung in Bayern im Rahmen der Geothermie-Allianz Bayern.  | 0.4<br>0.1<br>5·7        | 2<br>O |
| 84<br>83<br>82<br>81                               | Wellbore/borehole stability in shale formation. 2022, 125-154  Testing and Numerical Simulations on Fracture Behavior of Fresh Quartzite Rock Using the Discrete Element Method. Lecture Notes in Mechanical Engineering, 2022, 183-193  Rock Mechanical Basics. Springer Theses, 2022, 21-44  Mechanical and Fracture Behaviors of Brittle Material with a Circular Inclusion: Insight from Infilling Composition. Rock Mechanics and Rock Engineering, 1  Geomechanische Reservoircharakterisierung in Bayern im Rahmen der Geothermie-Allianz Bayern. Geomechanik Und Tunnelbau, 2022, 15, 27-36  Inducing Tensile Failure of Claystone Through Thermal Pressurization in a Novel Triaxial Device. | 0.4<br>0.1<br>5.7<br>0.6 |        |

| 76 | Evolutionary Analysis of Heterogeneous Granite Microcracks Based on Digital Image Processing in Grain-Block Model <i>Materials</i> , <b>2022</b> , 15,  | 3.5 | О |
|----|---|-----|---|
| 75 | Hydrodynamic and Geostress Controls on CBM Enrichment in the Anze Block, Southern Qinshui<br>Basin, North China. <i>Geofluids</i> , <b>2022</b> , 2022, 1-14  | 1.5 | 1 |
| 74 | Damage Characteristics of Thermally Deteriorated Carbonate Rocks: A Review. <i>Applied Sciences</i> (Switzerland), <b>2022</b> , 12, 2752   | 2.6 | 2 |
| 73 | Cracking and deformation of cuboidal sandstone with a single nonpenetrating flaw under uniaxial compression. <i>Theoretical and Applied Fracture Mechanics</i> , <b>2022</b> , 119, 103284              | 3.7 | 6 |
| 72 | New granular rock-analogue materials for simulation of multi-scale fault and fracture processes. <i>Geological Magazine</i> , 1-24  | 2   | O |
| 71 | Damage evaluation and precursor of sandstone under the uniaxial compression: Insights from the strain-field heterogeneity <i>PLoS ONE</i> , <b>2021</b> , 16, e0262054                                  | 3.7 | O |
| 70 | Dike Propagation During Global Contraction: Making Sense of Conflicting Stress Histories on Mercury. <i>Frontiers in Earth Science</i> , <b>2021</b> , 9,   | 3.5 | O |
| 69 | Use of Mohr Diagrams to Predict Fracturing in a Potential Geothermal Reservoir. <i>Geosciences</i> (Switzerland), <b>2021</b> , 11, 501   | 2.7 | O |
| 68 | Experimental Study on the Mechanical Characteristics of Single-Fissure Sandstone Under Triaxial Extension. <i>Rock Mechanics and Rock Engineering</i> , 1   | 5.7 | 1 |
| 67 | Depositional and diagenetic controls on the mechanical properties of rocks in the Monterey Formation of the Santa Maria Basin, California. <b>2022</b> ,  |     |   |
| 66 | Research on the failure mechanism and control technology of surrounding rock in gob-side entry driving under unstable overlying strata. <i>Engineering Failure Analysis</i> , <b>2022</b> , 138, 106361 | 3.2 | O |
| 65 | Characterization of Arching Effect and Failure Mode of longwall panel Floor. <i>Engineering Failure Analysis</i> , <b>2022</b> , 106427   | 3.2 | O |
| 64 | Effect of rock loading rate based on crack extension and propagation. Scientific Reports, 2022, 12,   | 4.9 | О |
| 63 | Simulation of hard rock pillar failure using 2D continuum-based Voronoi tessellated models: The case of Quirke Mine, Canada. <i>Computers and Geotechnics</i> , <b>2022</b> , 148, 104808               | 4.4 |   |
| 62 | Fracture mechanisms of intact rock-like materials under compression. <i>Computers and Geotechnics</i> , <b>2022</b> , 148, 104845   | 4.4 | O |
| 61 | Accurate experimental determination of rock fracture toughness under simulated reservoir confining pressures. <i>Theoretical and Applied Fracture Mechanics</i> , <b>2022</b> , 120, 103425             | 3.7 | O |
| 60 | A Comparative Study on Damage Variable and Geo-Mechanical Properties of the Pre-Damaged Rock Specimen. <i>Advances in Civil Engineering</i> , <b>2022</b> , 2022, 1-14                                  | 1.3 | O |
| 59 | Progressive Transition from Extension Fracture to Shear Fracture of Altered Granite During Uniaxial Tensile Tests. <i>Rock Mechanics and Rock Engineering</i> ,   | 5.7 | O |

| 58 | Effect of natural defects on the fracture behaviors and failure mechanism of basalt through mesotesting and FDEM modeling. <i>Engineering Fracture Mechanics</i> , <b>2022</b> , 271, 108598  | 4.2            |   |  |
|----|---|----------------|---|--|
| 57 | Modelling local failure around hard-rock tunnels based on a linked multiscale mesh strategy.  Tunnelling and Underground Space Technology, 2022, 127, 104588  | 5.7            | O |  |
| 56 | Experimental Investigation on Uniaxial Compressive Strength of Thin Building Sandstone. <i>SSRN Electronic Journal</i> ,  | 1              |   |  |
| 55 | An Instability Line for Spalling Around Circular Openings and the Limiting Effects of Scale. <i>Rock Mechanics and Rock Engineering</i> ,   | 5.7            |   |  |
| 54 | Research on uniaxial compression strength and failure properties of stratified rock mass. <i>Theoretical and Applied Fracture Mechanics</i> , <b>2022</b> , 103499  | 3.7            | 1 |  |
| 53 | Investigation into Rock Breakage with Expansive Cement Under Biaxial Confinement. <i>Rock Mechanics and Rock Engineering</i> ,  | 5.7            |   |  |
| 52 | Experimental investigation of the strain rate effect on crack initiation and crack damage thresholds of hard rock under quasi-static compression. <i>Acta Geotechnica</i> ,   | 4.9            | 1 |  |
| 51 | Estimating size of finite fracture networks in layered reservoirs. <i>Applied Computing and Geosciences</i> , <b>2022</b> , 15, 100089  | 2.8            | 1 |  |
| 50 | A new method for introducing plastic zone and tangential stress into tunnelling strain rockburst prediction. <i>Geotechnique Letters</i> , <b>2022</b> , 12, 1-34   | 1.7            |   |  |
| 49 | Determining Young's modulus of granite using accurate grain-based modeling with microscale rock mechanical experiments. <i>International Journal of Rock Mechanics and Minings Sciences</i> , <b>2022</b> , 157, 1051               | 6 <del>9</del> | 1 |  |
| 48 | Experimental investigation on rockburst process and characteristics of a circular opening in layered rock under three-dimensional stress conditions. <i>Tunnelling and Underground Space Technology</i> , <b>2022</b> , 127, 104603 | 5.7            | 1 |  |
| 47 | Microscopic and Acoustic Interpretations of the Physics of Rock Burst and the Difference in Fracturing Patterns in Class I and Class II Rocks.  |                | 1 |  |
| 46 | Experimental and numerical studies of a three-dimensional bonded contact model of cemented granular soils.  |                |   |  |
| 45 | Shear characteristics and shear strength model of rock mass structural planes. <b>2022</b> , 12,  |                |   |  |
| 44 | Study on crack growth behaviour in rocks having pre-existing narrow flaws under biaxial compression.  |                |   |  |
| 43 | Deformation and Failure Characteristics of Loading and Unloading Rock Based on Volume Crack Strain. 10,   |                |   |  |
| 42 | Confined Tensile Testing of Porous Sandstone.   |                |   |  |
| 41 | Dynamic mechanical behavior of rocks containing double elliptical inclusions at various inclination angles. <b>2022</b> , 121, 103544   |                | 1 |  |

| 40 | Mechanical responses of freezethaw treated natural stone masonry subject to compressive variable amplitude fatigue loading: Insights from stiffness loss and constitutive characterization. <b>2022</b> , 350, 128908 | O |
|----|---|---|
| 39 | Discrete element study on the mechanical behavior of flawed rocks under dynamic compression. <b>2022</b> , 121, 103516  | O |
| 38 | Mechanical properties and fracture mode transformation of rocks subjected to asymmetric radial stresses. <b>2022</b> , 81,  | 0 |
| 37 | Mechanical behavior of single-flawed cylindrical specimens subjected to axial loading: a numerical investigation. <b>2022</b> , 81,   | O |
| 36 | Study on the tensile-shear mechanical behavior of sandstone using a simple auxiliary apparatus. <b>2022</b> , 103608  | 0 |
| 35 | Fundamental physics distinguishes the initial stage acoustic emission (AE) behavior between compressive and fracture toughness tests in rock. <b>2022</b> , 275, 108829   | O |
| 34 | Griffith-based analysis of crack initiation location in a Brazilian test. <b>2022</b> , 159, 105227   | 0 |
| 33 | Numerical Analysis of Pillar Stability in Longwall Mining of Two Adjacent Panels of an Inclined Coal<br>Seam. <b>2022</b> , 12, 11028   | O |
| 32 | An experimental study of the transition from tensile failure to shear failure in Carrara marble and Solnhofen limestone: Does Bybrid failurelexist?. <b>2022</b> , 229623   | 0 |
| 31 | Fracture Mechanism of Crack-Containing Strata under Combined Static and Harmonic Dynamic Loads Based on Extended Finite Elements. <b>2022</b> , 15, 7940  | 1 |
| 30 | Effect of loading rate and time delay on the tangent modulus method (TMM) in coal and coal measured rocks. <b>2022</b> , 9,   | 0 |
| 29 | Experimental investigation on the effect of preexisting orthogonal cross flaws on cracking behaviors and acoustic emission characteristics of red sandstone. <b>2022</b> , 122, 103634                                | 0 |
| 28 | Experimental Investigation on Uniaxial Compressive Strength of Thin Building Sandstone. 2022, 12, 1945  | 0 |
| 27 | Finding the right place in Mohr circle space: Geologic evidence and implications for applying a non-linear failure criterion to fractured rock. <b>2023</b> , 166, 104773   | O |
| 26 | Analysis of Optimal Loading Angle in Dynamic Flattened Brazilian Disc Splitting Test for Concrete. <b>2022</b> , 12, 11834  | 1 |
| 25 | Structural control within flawed rock specimens under external loading as visualized through repeating nucleation on multiple sites by acoustic emission (AE). <b>2022</b> , 233, 490-509                             | O |
| 24 | Numerical Simulation of Curvature and Confining Pressure Effect on Progressive Failure of Surrounding Rock in Arch Tunnel with Straight Wall. <b>2022</b> , 2381, 012024  | 0 |
| 23 | Microstructure-Based Computational Analysis of Deformation Stages of Rock-like Sandy-Cement Samples in Uniaxial Compression. <b>2023</b> , 16, 24   | O |

| 22 | Methodology for the estimation of expansive cement borehole pressure. 2022,  | O |
|----|--|---|
| 21 | Rockburst process and strength-weakening effect of the high-stress circular tunnel under internal unloading. <b>2022</b> ,   | O |
| 20 | Preparative Knowledge of Material Properties. <b>2023</b> , 67-148   | О |
| 19 | An FE Simulation of the Fracture Characteristics of Blunt Rock Indenter Under Static and Harmonic Dynamic Loadings Using Cohesive Elements.  | O |
| 18 | Experimental Study on Rockburst and Spalling Failure in Circular Openings for Deep Underground Engineering.  | O |
| 17 | Quakes of Compact Stars.   | O |
| 16 | Rheology and breakdown energy of a shear zone undergoing flash heating in earthquake-like discrete element models. <b>2023</b> , 233, 1492-1514  | 0 |
| 15 | Spatial Characterization of Single-Cracked Space Based on Microcrack Distribution in Sandstone Failure. <b>2023</b> , 13, 1462   | O |
| 14 | Brittle-ductile transition stress of different rock types and its relationship with uniaxial compressive strength and Hoek <b>B</b> rown material constant (mi). <b>2023</b> , 13,     | O |
| 13 | Influence of the Hoek <b>B</b> rown failure criterion with tensile strength cut-off on the roof stability in deep rock tunnels. <b>2023</b> , 136, 105016                              | O |
| 12 | Ductile Deformation of the Lithospheric Mantle. <b>2023</b> , 51,  | 0 |
| 11 | Micro-scale Fracturing Mechanisms in Rocks During Tensile Failure.   | O |
| 10 | Evaluating the Effect of Overburden Depth, Mining Height, and Support Density on Coal Rib Damage Using DEM Modeling. <b>2023</b> , 13, 77  | O |
| 9  | Nonlinear strain energy based (NSEB) criterion for quasi-brittle materials under multiaxial stress states. <b>2023</b> , 375, 131001   | O |
| 8  | Stability Evaluation of Rock Slopes with Cracks Using Limit Analysis.  | O |
| 7  | Quantitative Identification of Mesoscopic Failure Mechanism in Granite by Deep Learning Method Based on SEM Images.  | O |
| 6  | Energy Behaviour of Coal Failure under Uniaxial Cyclic Loading/Unloading. 2023, 13, 4324   | O |
| 5  | Role of Inherited Tectonic Structures on Gravity-Induced Slope Deformations: Inference from Numerical Modeling on the Luco dei Marsi DSGSD (Central Apennines). <b>2023</b> , 13, 4417 | O |

Macro and micro investigation of fracture behavior and crack evolution considering inherent microcrack in prefabricated flawed granite. 2023, 284, 109264

Influence of coplanar double fissures on failure characteristics of sandstone and fracture mechanics analysis. 11,

A nonlinear constitutive model for whole stressEtrain behaviors of compressed rocks incorporating crack closure effect.

O

Experimental study on mode I fracture characteristics of compacted bentonite clay. 2023, 285, 109294

o